Accessibility of the CLC-0 Pore to Charged Methanethiosulfonate Reagents

Xiao-Dong Zhang, Wei-Ping Yu, and Tsung-Yu Chen*
Center for Neuroscience and Department of Neurology, University of California, Davis, California

ABSTRACT Using the substituted-cysteine-accessibility method, we previously showed that a cysteine residue introduced to the Y512 position of CLC-0 was more rapidly modified by a negatively charged methanethiosulfonate (MTS) reagent, 2-sulfonatoethyl MTS (MTSES), than by the positively charged 2-(trimethylammonium)ethyl MTS (MTSET). This result suggests that a positive intrinsic pore potential attracts the negatively charged MTS molecule. In this study, we further test this hypothesis of a positive pore potential in CLC-0 and find that the preference for the negatively charged MTS is diminished significantly in modifying the substituted cysteine at a deeper pore position, E166. To examine this conundrum, we study the rates of MTS inhibitions of the E166C current and those of the control mutant current from E166A. The results suggest that the inhibition of E166C by intracellularly applied MTS reagents is tainted by the modification of an endogenous cysteine, C229, located at the channel's dimer interface. After this endogenous cysteine is mutated, CLC-0 resumes its preference for selecting MTSES in modifying E166C, reconfirming the idea that the pore of CLC-0 is indeed built with a positive intrinsic potential. These experiments also reveal that MTS modification of C229 can inhibit the current of CLC-0 depending on the amino acid placed at position 166.

INTRODUCTION

CLC-0 from the electric organ of *Torpedo* rays is a voltage-dependent Cl^- channel in the CLC channel/transporter family (1–5). Although several CLC family members are suggested to be Cl^--H^+ antiporters (6–8), CLC-0 is a Cl^- channel, with a Cl^- flux rate through the channel pore on the order of 10^7 ions per second. The opening and closing of the CLC-0 pore is controlled by two gating mechanisms, termed the ''fast-gating'' and ''slow-gating'' mechanisms (1,4,9). Though the relationship between the CLC-0 gating mechanisms and the Cl^--H^+ antiporter mechanism of the bacterial CLC molecule (such as CLC-ec1) is not clear, the structural architectures of all CLC proteins appear to be conserved (3,4). For example, high-resolution structures of bacterial CLCs show the obstruction of the Cl^- transport pathway by a glutamate residue, E148 (10,11). Mutation of the corresponding glutamate (E166) of CLC-0 to alanine or glutamine results in a constantly open channel, leading to the hypothesis that the negatively charged side chain of this residue acts as the fast gate of CLC-0 (11).

In addition to the aforementioned conserved glutamate residue, several lines of experiments also indicate that the high-resolution structure of bacterial CLC molecules provides a good roadmap for studying eukaryotic CLC proteins. Experiments employing fluorescence resonance energy transfer (FRET) techniques suggested that the distance between the C-terminal end of helix R in CLC-0 is comparable to that in CLC-ec1 (12). Furthermore, cysteine modification experiments using methanethiosulfonate (MTS) reagents also showed a similarity in the structural architecture of CLC-0 and bacterial CLCs (13–15). For example, MTS modification of cysteine residues along helix R of CLC-0 revealed a helical pattern as shown by the bacterial CLC structure (13). MTS modification experiments also showed that compared to the positively charged reagent, the negatively charged MTS was favored in the modification of the cysteine introduced into the pore, as if the pore had an intrinsic positive potential (13,15).

In the previous modification experiments using intracellularly applied MTS reagents, the deepest probed position in the CLC-0 pore was Y512 (13), a residue only 4 Å away from E166 (10,11). Y512 and E166 appear to be in the narrowest region of the pore, according to the bacterial CLC structure (10,11). We recently used amphiphilic pore blockers, such as parachlorophenoxy acetate (CPA) and octanoate (Fig. 1 *A*), to block the CLC-0 pore and found that the side chain of the residue at position 166 interacts with negatively charged amphiphilic blockers (16). Accordingly, negatively charged MTS reagents, such as 2-sulfonatoethyl MTS (MTSES) and 5-sulfonatopentyl MTS (MTSPeS) (Fig. 1 *A*), can also reversibly block the pore of E166C (Fig. 1, *B* and *C*). On the other hand, a positively charged MTS reagent, such as 2-aminoethyl MTS (MTSEA), does not show a reversible block (Fig. 1 *B*). Surprisingly, the irreversible current inhibition of the E166C mutant, presumably due to cysteine modifications (17), is faster when MTSEA is used as the modifying reagent. To solve this puzzle, we compared the MTS modification rates of Y512C and E166C during various pore manipulations. Further experiments revealed that MTS reagents not only inhibited the E166C current, they also reduced the current of the E166A mutant. These results reveal a cytoplasmic cysteine residue at the dimer interface whose modification by the MTS reagents reduces the current of the channel depending on the residue placed at the 166 position.

Submitted May 26, 2009, and accepted for publication September 24, 2009.

*Correspondence: tycchen@ucdavis.edu

Editor: Tzyh-Chang Hwang.

0006-3495/10/02/0377/9 $2.00

doi: 10.1016/j.bpj.2009.09.066

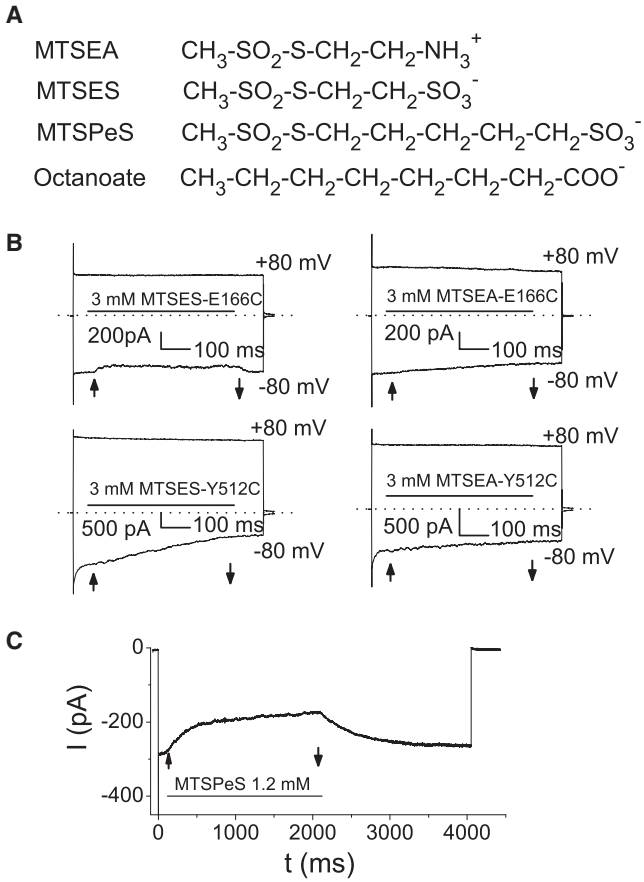

FIGURE 1 Negatively charged MTS reagents reversibly block the pore of the E166C mutant. (*A*) Molecular structure of MTS reagents and octanoate. (*B*) Comparison of the block of MTSES and MTSEA in the E166C (*upper panels*) and Y512C (*lower panels*) mutants. Recording traces were obtained by changing the voltage from 0 mV to +80 mV, and to −80 mV. Application of MTS reagents (3 mM for both MTSES and MTSEA) via a fast solution exchange is indicated by the horizontal bars (wash-in and washout of MTS reagents are also indicated by *arrows*). Notice that only the intracellular application of MTSES to the E166C mutant at −80 mV shows a reversible current inhibition in response to the fast solution exchange. (*C*) A longer, negatively charged MTS reagent (MTSPeS) is more potent in reversibly blocking E166C than MTSES. Notice that a lower concentration (1.2 mM) of MTSPeS generates a larger degree of steady-state block at −80 mV compared to the MTSES block shown in *B*.

MATERIALS AND METHODS

Mutagenesis and channel expression

All CLC molecules consist of two identical subunits, each of which contains a Cl^- transport pathway. In CLC-0, the fast-gating mechanism controls the individual protopore in the millisecond time range, whereas the slow-gating mechanism opens and closes the two protopores simultaneously on a timescale of seconds (1,9). For convenience, we designed the experiments so that the MTS modification rates would be in the range of several seconds. Therefore, locking the slow gate of CLC-0 in the open state simplified the data acquisition and analysis. For this purpose, we took advantage of a point mutant, C212S, whose channel properties are identical to those of the wild-type (WT) channel, except for a locked-open slow gate (18). Except when indicated otherwise, all of the mutations were constructed in the C212S mutation background, and the term "WT channel" refers to the C212S mutant. In the experiments illustrated in Fig. 5, we mutated endogenous cysteines both in groups and individually to identify the endogenous cysteine whose modification caused a functional consequence. Besides C212, there are 11 cysteine residues in the WT CLC-0 channel. The mutations were made using polymerase chain reaction mutagenesis approaches, and were confirmed by commercial DNA sequencing services. All cDNAs were constructed in the pcDNA3 vector for expression in human embryonic kidney (HEK) 293 cells. Transfection of cDNA into HEK 293 cells was performed as described previously (13,15). Normally, the experiments were performed 1–3 days after cDNAs were transfected into the HEK 293 cells.

Electrophysiological recordings

Macroscopic current recordings from the excised, inside-out membrane patches of HEK 293 cells were performed throughout the study, using previously described methods (13,15). Briefly, the experiments were conducted with the use of an Axopatch 200B amplifier (Axon Instruments/Molecular Devices, Union City, CA). The recording was digitally filtered at 1 kHz and digitized at 2 kHz using a Digidata 1320 digitizing board and pClamp8 software (Axon Instruments/Molecular Devices). The recording pipettes were pulled from borosilicate glass (World Precision Instruments, Sarasota, FL) using a vertical pipette puller (pp830; Narishige International, New York, NY). Except when indicated otherwise, the standard pipette and the bath solutions contained (in mM) 130 NaCl, 5 $MgCl_2$, 10 HEPES, 1 EGTA, pH 7.4. The pipette resistance was ~2–4 MΩ. For certain experiments, the Cl^- concentration ($[Cl^-]$) in the bath solution was changed. In these experiments, $MgCl_2$ was replaced with $MgSO_4$, and NaCl was replaced with NaGlu to make the desired $[Cl^-]$.

MTS modifications

MTS reagents (see Fig. 1 *A*) were purchased from Toronto Research Chemicals (North York, Canada). The stock solution of 0.3 M was first made in distilled water and then stored at −80°C. An aliquot of stock solution was placed on ice during the experiment. The working solutions containing the required MTS reagents were made immediately before use and were discarded if they were not used within 5 min.

MTS reagents were applied to the intracellular side of the excised membrane patches by means of an SF-77 solution-exchanger (Warner Instruments/Harvard Apparatus, Hamden, CT). The detailed modification protocol was described previously (13). Briefly, the membrane potential of the excised patch was clamped at particular voltages (V_{MO}) for 1.4 s, during which time the patch was exposed to the intracellularly applied MTS reagent for 1 s. Following the 1.4 s voltage step of V_{MO}, the voltage was stepped to +80 mV (V_{MN} = +80 mV) for 100 ms to measure the remaining current. This modification procedure was repeated every 2 s. The time constant of the current-inhibition process upon application of the MTS reagent was used to determine the MTS modification rate (k_{MTS}). The current measured at +80 mV at each recording sweep was normalized to that measured right before the start of MTS modification, as shown in Fig. 2 *A*. The MTS modification process was then fitted to a single-exponential function. The time constant (τ_{mo}) and the concentration of MTS reagents ([MTS]) were used to calculate the rate constant according to the following equation:

$$k_{MTS} = 1/(\tau_{mo} \times [MTS]). \quad (1)$$

For the purpose of presenting the averaged MTS modification process and comparing the modification processes in different conditions, the current-inhibition process, except for those shown in Fig. 5, is plotted against the accumulative exposure, i.e., concentration × time (with a unit of mM × s). Averaged data are presented as the mean ± SE (n = 3–6).

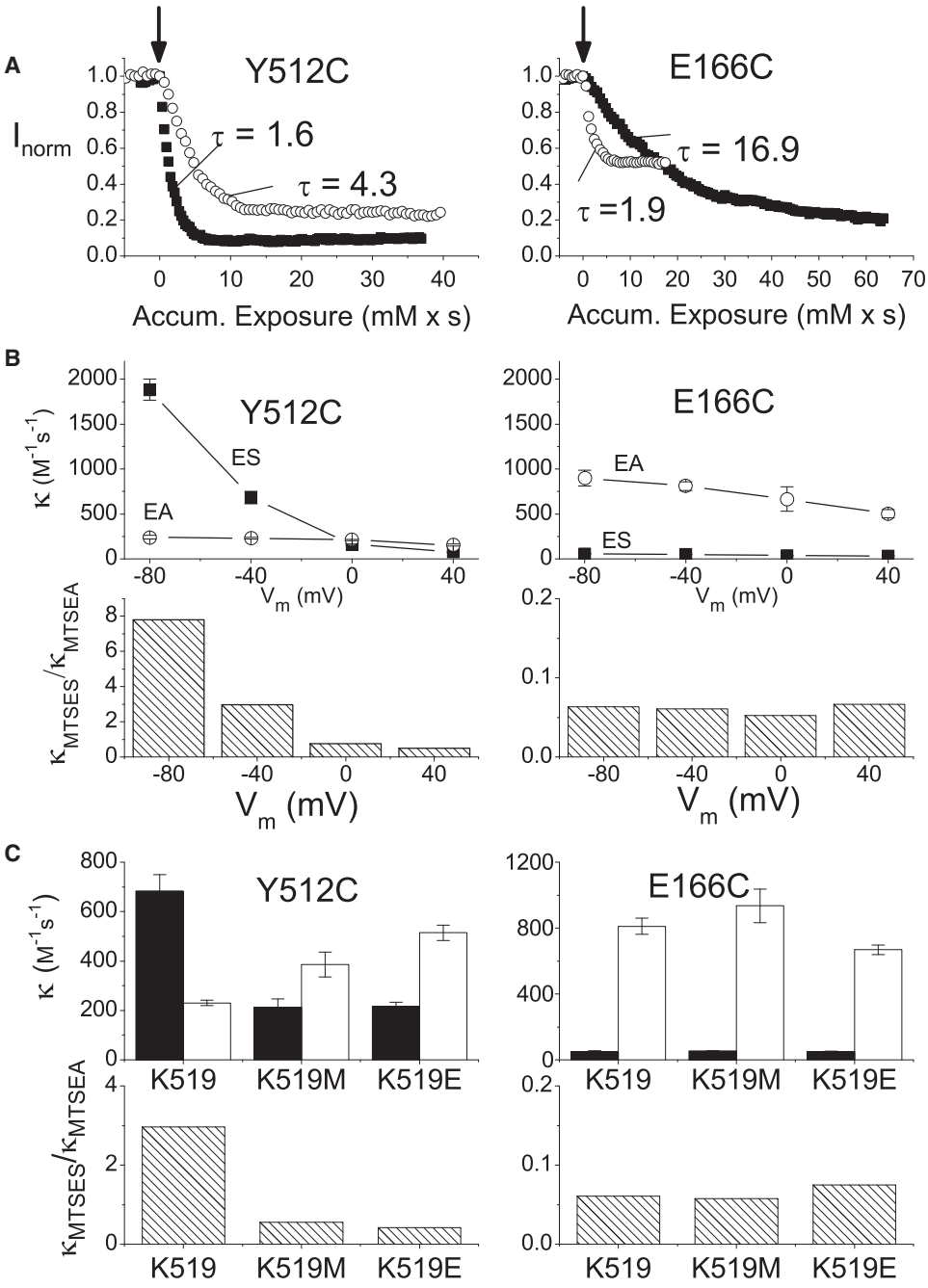

FIGURE 2 Comparison of the rate of modification of Y512C to that of E166C by MTSES and MTSEA. (*A*) Time course of the modification of Y512C (*left panel*) and E166C (*right panel*) by intracellularly applied MTSES (*solid symbols*) and MTSEA (*open symbols*). Excised inside-out patch recordings are shown; V_{MO} (duration 1400 ms) = −40 mV, and V_{MN} (duration 100 ms) = 80 mV. MTS reagents were applied as indicated by the downward arrows. The current amplitudes measured at V_{MN} from the recording traces were normalized to that obtained just before the application of MTS reagents. (*B*) Modification rates of Y512C and E166C by MTSES (*solid squares*) and MTSEA (*open circles*) at voltages from −80 mV to + 40 mV. The second-order rate constant was calculated from the measured time constant of the current inhibition course according to Eq. 1. Upper panels are modification rates at different voltages. Lower panels show the ratio of k_{MTSES}/k_{MTSEA} at various modification voltages. (*C*) Effects of K519 mutations on the MTS modification rates of Y512C and E166C. Upper panels are MTSES (*solid bars*) and MTSEA (*open bars*) modification rates at V_{MO} = −40 mV. Lower panels show the ratio of k_{MTSES}/k_{MTSEA}.

RESULTS

Negatively charged MTS reagents reversibly block E166C but not Y512C

Negatively charged pore blockers, such as CPA and fatty acids, are known to block CLC-0 reversibly. The blocking affinity of these amphiphilic compounds is increased dramatically if the residue E166 is replaced with a residue containing a small and/or hydrophobic side chain. For example, the apparent half-blocking affinity ($K_{1/2}$) of octanoate for the WT pore is ~0.7 mM at −80 mV, whereas the $K_{1/2}$ of octanoate for the E166C mutant is ~0.02 mM at the same voltage (16). On the other hand, the amphiphilic blocker with a shorter hydrophobic chain blocks E166C with a lower affinity—the $K_{1/2}$ of butyrate for the E166C mutant is >1 mM at −80 mV (16).

MTSES and MTSPeS both contain a negatively charged sulfonate on one end of the molecule. The rest of the molecule is an aliphatic-thiol chain ended with a methane thiol group (Fig. 1 *A*). It is therefore expected that these two compounds can reversibly block E166C, although their blocking affinities may be lower than that of octanoate because the aliphatic chain in fatty acids is more hydrophobic compared to the methane thiol group of MTS

reagents. Fig. 1, *B* and *C*, show that both MTSES and MTSPeS reversibly block the E166C mutant (indicated by *arrows*) at negative voltages, but not at positive voltages. On the other hand, the positively charged MTS reagent, MTSEA, does not produce a reversible block in E166C. Furthermore, because MTSPeS has a longer hydrophobic chain than MTSES (Fig. 1 *A*), the off-rate of the former is much slower than that of the latter, resulting in a higher steady-state blocking affinity for MTSPeS in blocking the pore of E166C. These results are consistent with our previously proposed blocking mechanism for amphiphilic molecules in CLC-0 (16).

MTSES and MTSEA irreversibly inhibit the current of E166C and Y512C

In addition to the reversible block described above, MTSES, as well as the positively charged reagent MTSEA, also irreversibly inhibits the current of the Y512C and E166C mutant channels (Fig. 2 *A*), presumably due to the modification of the cysteine residues on the channel. However, these two mutant channels have different preferences in favoring negatively or positively charged MTS molecules. At negative voltages the MTSES modification rate of Y512C is faster than that of MTSEA, whereas in the E166C mutant the preference of MTSES over MTSEA is reversed: the MTSES modification is slower than the MTSEA modification. Furthermore, the MTSES modification rate of Y512C is voltage-dependent, whereas the voltage dependence of the MTSES and MTSEA modifications in E166C is negligible. Therefore, the ratio of the MTSES and MTSEA modification rates (k_{MTSES}/k_{MTSEA}) ranges from ~0.5 to ~8 (from +40 mV to −80 mV) in Y512C, whereas the k_{MTSES}/k_{MTSEA} for E166C remains quite constant (~0.06) in the same voltage range (Fig. 2 *B*). Because the intrinsic reactivity of MTSEA is ~50-fold higher than that of MTSES, these results appear to suggest that the pore of the Y512C mutant channel favors the MTSES molecule, and this preference is greatly reduced in the E166C mutant (see Discussion).

The observation that Y512C, but not E166C, has a preference for a negatively charged MTS reagent over a positively charged MTS reagent is surprising because the positions of these two residues are both deep in the pore, separated by merely 4 Å. If the intrinsic potential is critical in determining the accessibility of the pore to charged MTS reagents (13,15), these two mutants should have a similar k_{MTSES}/k_{MTSEA} ratio. Previous studies revealed that two charged residues, K519 and E127, are critical for the channel conductance, possibly due to its electrostatic control of the intrinsic potential at the intracellular pore entrance (13,19,20). We therefore tested the effect of K519/E127 mutations on the MTS modification in Y512C and E166C. Consistent with previous studies, the k_{MTSES}/k_{MTSEA} ratio of Y512C indeed depends on the charge at position 519—the ratio decreases with a less positive charge at this position (Fig. 2 *C*, *left*). This electrostatic effect is suppressed by a simultaneous E127Q mutation (data not shown). On the other hand, the k_{MTSES}/k_{MTSEA} ratio for the E166C modification is not affected by K519 mutations (Fig. 2 *C*, *right*). The k_{MTSES}/k_{MTSEA} ratio of the E166C mutant remains the same whether a positively charged lysine or a negatively charged glutamate is located at this position.

Pore manipulations affect the MTSES modification of Y512C but not E166C

The negligible effect of K519 mutations on the E166C modification led us to suspect that the irreversible current inhibition of E166C by MTS reagents may not be due to the modification of the introduced cysteine at position 166. If the modification indeed occurs in the pore, we would expect the pore manipulations to affect the modification in a predicted manner. Accordingly, we further tested the MTSES modifications in Y512C and E166C under two manipulations: altering the intracellular Cl^- concentration ($[Cl^-]_i$) and blocking the pore with CPA, a CLC-0 pore blocker (16,21). Fig. 3, *A* and *B* show that increasing $[Cl^-]_i$ reduces the MTSES modification rate in Y512C but not in E166C. Similarly, intracellular application of 3 mM CPA to block the channel also reduces the MTSES modification rate in Y512C but not in E166C. Because Cl^- and CPA are known to enter the pore, the presence of Cl^- and CPA is likely to compete with the modifying MTSES molecule and reduce the MTSES modification rate. However, neither pore manipulation affects the MTSES modification rate of E166C in a predicted manner. These results suggest that perhaps the modification of an endogenous cysteine contributes to the current inhibition of E166C.

MTS reagents irreversibly inhibit the E166A mutant

If the inhibition of the current of E166C by MTS modification is not due purely to the modification of cysteine at position 166, MTS reagents may still be able to irreversibly inhibit E166 mutants other than E166C. Even though the MTS reagents produce very little effect when the WT residue glutamate is at position 166 (Fig. 4 *A*), this possibility cannot be excluded when other amino acids are placed at this position. Accordingly, we compared the MTSES and MTSEA modifications of E166A to those of the E166C mutant (Fig. 4, *B* and *C*). It can be seen that both MTSES and MTSEA are able to irreversibly inhibit E166C and E166A mutants. The MTSES modification rate is only slightly reduced in the E166A mutant compared to that of E166C, whereas the MTSEA modification rates in the E166C and E166A mutants are nearly the same. These results clearly demonstrate that modification of an endogenous cysteine is responsible for the irreversible inhibition of E166A by MTS reagents, suggesting that the MTS modification rate of E166C may be tainted by the modification of the endogenous cysteine.

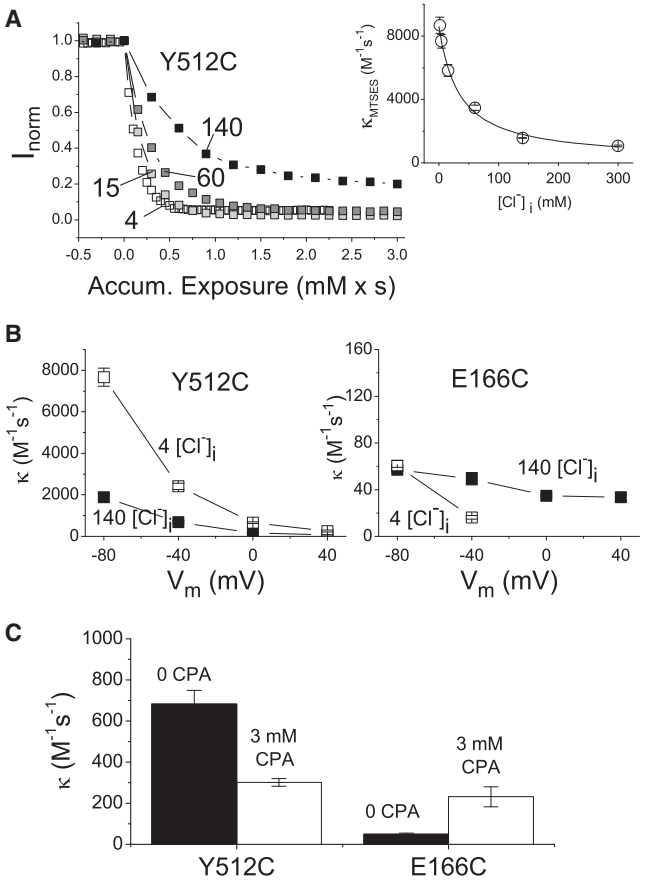

FIGURE 3 Inhibition of Y512C by MTSES is mostly due to modification activity in the pore, but modification of E166C may include a cysteine modification outside the pore. (*A*) The MTSES modification time course of Y512C depends on $[Cl^-]_i$. Numbers represent $[Cl^-]_i$ (in mM) in each modification. Inset: MTSES modification rate of Y512C as a function of $[Cl^-]_i$. The solid curve is the best fit to a hyperbolic equation: $k_{MTSES} = P_2 + (P_1 - P_2)/(1 + [Cl^-]/K_{1/2})$, with $P_1 = 8605\ M^{-1}s^{-1}$, $P_2 = 181\ M^{-1}s^{-1}$, and an apparent half-effective Cl^- concentration ($K_{1/2}$) of 33 mM. (*B*) MTSES modification rates of Y512C (*left*) and E166C (*right*) in two $[Cl^-]_i$. (*C*) Intracellular pore blocker reduces k_{MTSES} of Y512C but increases that of E166C.

Modification of C229 is responsible for the MTS inhibition of E166A

To search for the endogenous cysteine, we constructed mutations of endogenous cysteine residues in the background of the E166A mutation. We used MTSEA to explore the modification because MTSEA had a more robust irreversible inhibition on E166A than MTSES. Fig. 5 *A* shows our initial screen, in which a mutant construct may contain multiple cysteine mutations. It can be seen that the mutant channel containing three cysteine mutations (C212A, C213A, and C229S) is resistant to the MTSEA-induced current inhibition. Because the E166A mutant in the WT background referred to in this study (containing the C212S mutation) is inhibited by MTSEA, the target could only be C213 or C229. As can be seen from Fig. 5 *B*, although the C213A/C212S double mutant is still sensitive to MTSEA modification, the C229S/C212S mutant is resistant to MTSEA modification. We conclude that the modification of C229 is responsible for the MTS inhibition in the E166A mutant, and this modification could also contribute to the irreversible inhibition of the E166C current.

C229S mutation resumes a higher MTSES accessibility in modifying E166C

As shown in Fig. 4, *B* and *C*, replacing cysteine with alanine at position 166 only slightly reduced the MTSES modification rate, and had no effect on the MTSEA modification rate. We suspected that the MTS modification of C229 must significantly contribute to the MTS-induced current inhibition of E166C. To evaluate more precisely the modification rate of the cysteine at position 166, we modified the E166C mutant in the background of the C229S mutation. As shown in Fig. 6, both MTSES (Fig. 6 *A*) and MTSEA (Fig. 6 *B*) can still irreversibly inhibit the E166C/C229S mutant. On the other hand, both MTSES and MTSEA have very little effect on the E166A/C229S mutant. For the E166C/C229S mutant, neither the charge mutation (K519M) at the pore entrance (Fig. 6 *C*) nor the change of the membrane voltage (Fig. 6 *D*) alters the MTS modification rates. The MTSES modification rate of E166C/C229S is not significantly different from that of E166C (shown in Fig. 4). However, the MTSEA modification rate of E166C/C229S is reduced by removing the MTS modification target at position 229. The resulting k_{MTSES}/k_{MTSEA} ratio in the E166C/C229S mutant is ~0.7. Because the intrinsic reactivity of MTSEA is >50-fold higher than that of MTSES, a k_{MTSES}/k_{MTSEA} ratio of 0.7 reflects a higher accessibility of MTSES over MTSEA by ~35-fold in reaching the cysteine at the 166 position.

DISCUSSION

This study was motivated by the observation that the ratios of the MTSES and MTSEA modification rate constants, k_{MTSES}/k_{MTSEA}, are very different for the cysteine at two nearby positions in the CLC-0 pore, namely, Y512C and E166C. The k_{MTSES}/k_{MTSEA} ratio for a pore cysteine can reflect the intrinsic electrostatic potential in the channel pore (13,22,23). It has been reported that the reaction rates of MTSEA and MTSES with β-mercaptoethanol in aqueous solutions are ~5 × 10^5 $M^{-1}s^{-1}$ and 10^4 $M^{-1}s^{-1}$, respectively, suggesting that the intrinsic reactivity of MTSEA is ~50-fold greater than that of MTSES (24). Thus, a k_{MTSES}/k_{MTSEA} ratio of 1 may reflect a 50-fold accessibility advantage for the negatively charged MTSES molecule over the positively charged MTSEA molecule. Our results show that the k_{MTSES}/k_{MTSEA} ratio of the Y512C modification is 0.5–8 within the voltage range of +40 mV to −80 mV, indicating that MTSES is favored by 25- to 400-fold over MTSEA in reaching the cysteine at the Y512 position. On the other hand, the k_{MTSES}/k_{MTSEA} ratio of E166C has a constant value of ~0.06 within the tested voltage range,

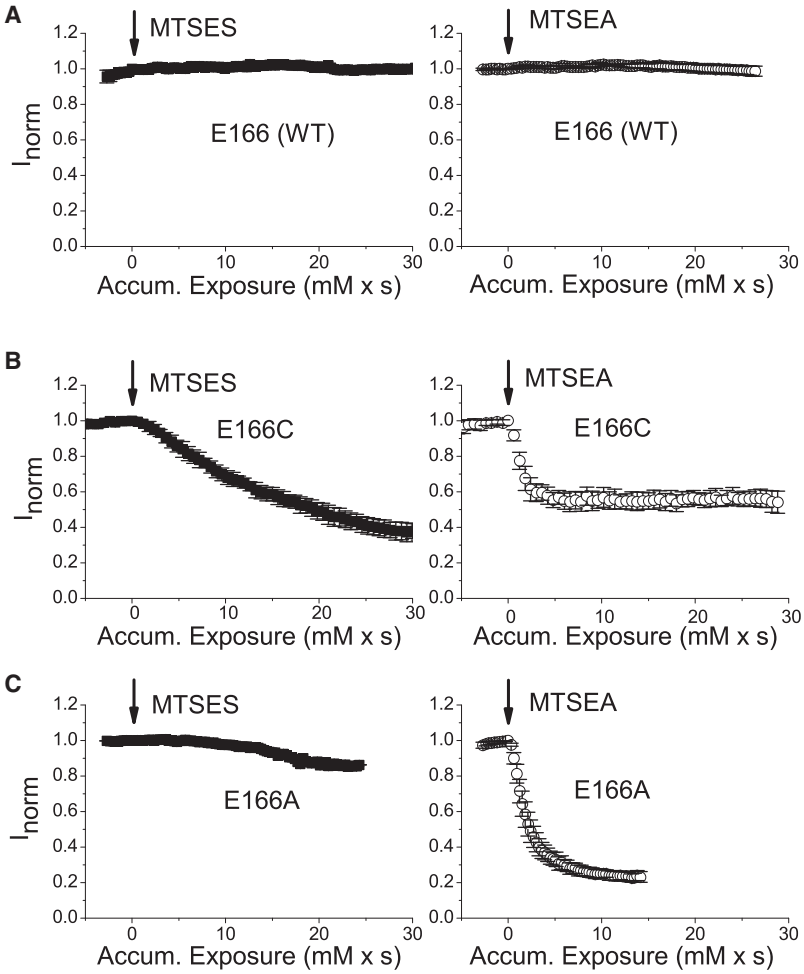

FIGURE 4 Comparison of the MTSES and MTSEA modification rates of CLC-0 in which (*A*) glutamate, (*B*) cysteine, and (*C*) alanine are located at position 166. Downward arrows indicate the beginning of the application of MTS reagents.

suggesting that the preference of MTSES over MTSEA is greatly lost in modifying this mutant channel. Because E166 and Y512 are very close to each other in the pore (within a distance of only 4 Å), it is quite surprising that the k_{MTSES}/k_{MTSEA} ratios of E166C and Y512C differ from each other so dramatically.

Because altering charged residues in the pore region did not affect the modification pattern of E166C by MTSES

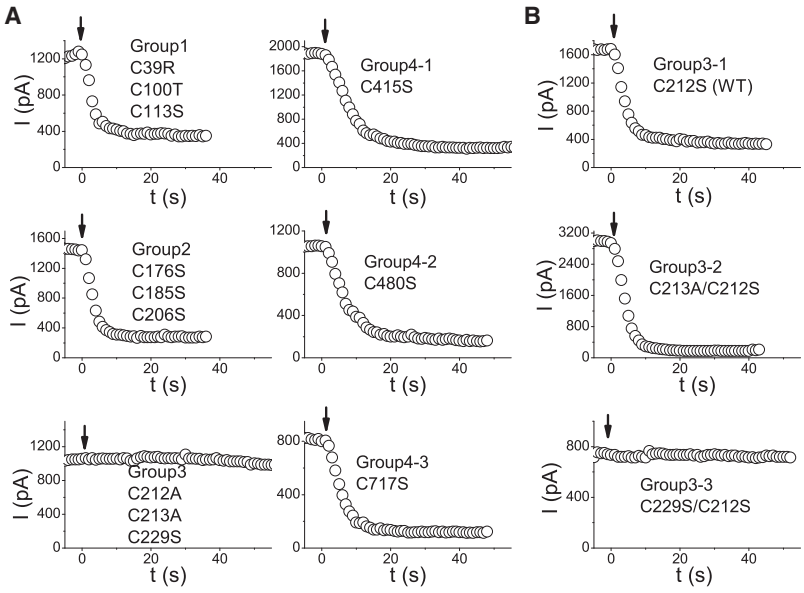

FIGURE 5 Searching for the endogenous cysteine responsible for the current inhibition caused by MTS modifications. All cysteine mutants were constructed in the background of the E166A mutation. MTSEA is 300 μM in all panels, which depict the experiments in single patches. (*A*) Examples of MTSEA modifications of cysteine-removed mutants of CLC-0. The 12 endogenous cysteine residues are divided into four groups, each of which encompasses three cysteine residues. All three cysteine residues are removed simultaneously for the first three groups, and the individual cysteine residue is mutated one by one for the fourth group. MTSEA was applied as indicated by the arrows. (*B*) Searching for the cysteine residue in group 3 responsible for the lack of inhibition by the MTSEA modification.

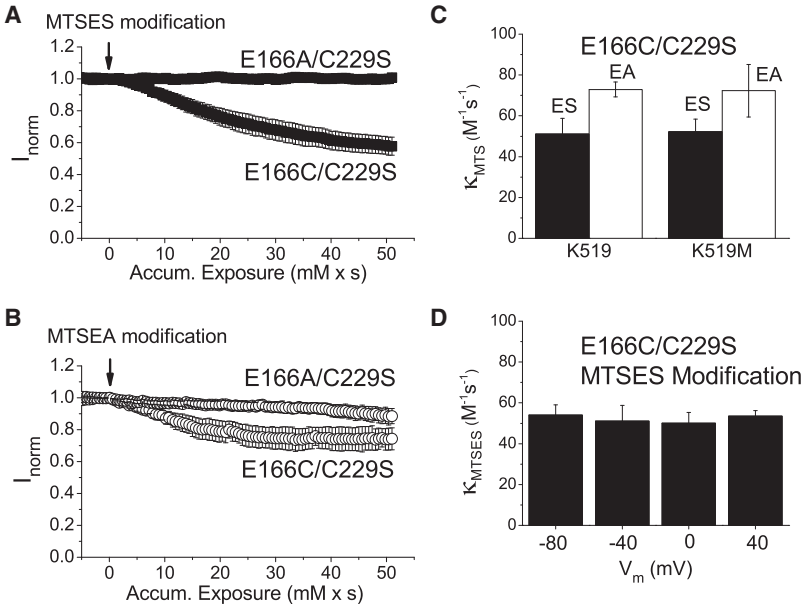

FIGURE 6 Comparison of the MTSES and MTSEA modification rates in the E166C/C229S-related mutants. (*A* and *B*) Current-inhibition course of the E166C/C229S mutant by MTSES (*A*) and MTSEA (*B*). For comparison, MTS modifications of E166A/C229S are also shown. (*C*) Averaged MTSES (*solid bars*) and MTSEA (*open bars*) modification rates of the E166C/C229S (labeled as K519) and E166C/C229S/K519M (labeled as K519M) mutants. (*D*) Averaged MTSES modification rates of the E166C/C229S mutant at four voltages.

and MTSEA (Fig. 2 *C*), we suspected that the MTS-induced, irreversible current inhibition of E166C might not be due purely to the modification in the pore. We thus tested the effects of two manipulations on the MTS modification rates: varying $[Cl^-]_i$ and blocking the pore with CPA (Fig. 3). Both Cl^- and CPA carry a negative charge and can enter the pore of CLC-0. The occupancy of the pore with Cl^- or CPA should inhibit the binding of the negatively charged MTSES in the pore and thus reduce the MTSES modification rate. This expectation was valid in Y512C but not in E166C. Furthermore, MTS reagents still irreversibly inhibited the current of the E166A mutant (Fig. 4 *C*). This latter observation indicates that MTS modification of an endogenous cysteine causes the irreversible current inhibition in the E166A mutant.

By testing whether MTSEA modification can reduce the current in various cysteine mutants, we were able to determine that C229, which is located at the loop between helix H and helix I at the dimer interface of CLC-0, can be modified by MTS reagents (Fig. 5). However, the electrophysiological approach can only report a cysteine whose modification leads to a functional consequence. Therefore, we cannot rule out the modification of other endogenous cysteines by intracellularly applied MTS reagents. Nonetheless, modification of C229 by MTS reagents can lead to a current reduction in the E166A mutant. The C229 modification also appears to contribute to the current reduction of the E166C mutant, as can be seen by comparing the currents after MTS modification of E166C to that of the E166C/C229S double mutant—eliminating the cysteine at position 229 reduces both the MTSES and MTSEA modification effects (Fig. 6). Because modification of C229 contributes to the current inhibition, the current inhibition of E166C reflects at least the summation of the modification of cysteine residues at positions 166 and 229. On the other hand, the modification of the E166C/C229S mutant should represent a better estimate of the modification rate of the cysteine at position 166. The k_{MTSES}/k_{MTSEA} ratio of the E166C/C229S mutant is ~0.7, a value that reflects a ~35-fold selection of MTSES over MTSEA in accessing the cysteine residue at position 166. These results indeed support the hypothesis that the pore of CLC-0 has a positive intrinsic potential.

It is interesting that MTS modification of C229 appears to have little effect in reducing the current when a glutamate residue is at position 166 (Fig. 4 *A*). Thus, the functional consequence of modifying a cysteine at the dimer interface depends on a residue in the pore. We suspect that this could come from an allosteric structural communication between the pore region near residue 166 and the region near C229 at the dimer interface. A recent study by Osteen and Mindell (25) also suggested an allosteric communication between residue 166 and an extracellular Zn^{2+}-binding site in CLC-4 through the movement of helix N. It will be interesting to further explore the movement transmitted from the dimer interface to the pore region, a possible mechanism underlying the slow-gating mechanism of CLC-0 (12).

One difference between Y512C and E166C is that the MTSES modification of the former is much more voltage-dependent. The voltage dependence is expected if the Cl^- occupancy in the pore is less at more negative membrane potentials (26,27) and/or if the binding of the negatively charged MTSES molecule to the pore follows the Woodhull-type voltage-dependent mechanism (28). However, these explanations alone cannot explain the difference in voltage dependence between the E166C and Y512C modifications. It should be noted that the off-rate of MTSES (or MTSPeS) is likely much smaller in the E166C pore than in the Y512C pore because the side chain of cysteine

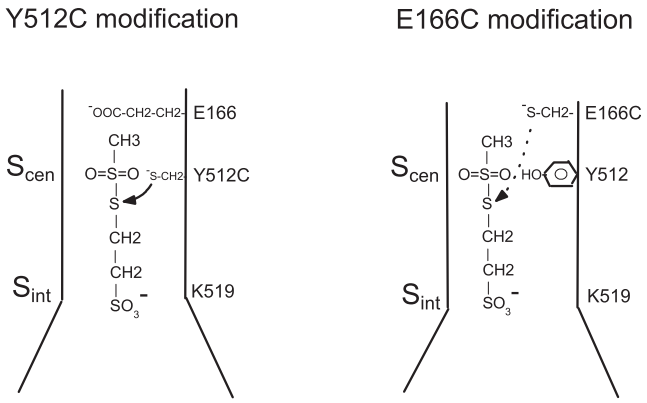

FIGURE 7 Hypothetical diagram depicting the position of the MTSES molecule with respect to the three pore residues when Y512C (*left*) or E166C (*right*) is modified. Only one pore of the double-barreled channel is shown. The extracellular end of the pore is on top. S_{cen} and S_{int} respectively represent the central and internal Cl^- binding sites observed in the bacterial CLC molecule. Because the side chain of the residue at position 166 (whether it is glutamate or cysteine (21)) does not allow the punch-through of MTSES, the location of the bound MTSES does not easily allow the MTS end to reach the thiol group at position 166 (*dotted curved arrow* on the *right panel*). On the other hand, the orientations of the MTS group and the thiol at position 512 should help the reaction occur more easily (*solid curved arrow* on the *left panel*).

at position 166, compared to that of glutamate (in the Y512C mutant), has a tighter interaction with MTS molecules (16). Yet, the absolute MTSES modification rate of Y512C is larger than that of the E166C mutant, at least in the negative voltage range (Fig. 2 *B*). We suspect that the sluggish rate of modifying E166C is the result of structural constraints in the pore. Because the side chain of the amino acid (other than glycine) at position 166 prevents the punch-through of the MTS molecule (21), residue 166 is likely to be the deepest position that intracellularly applied MTS reagents can reach. Fig. 7 depicts our vision of the bound MTSES molecule in the pore. It is quite straightforward to see that such a location of the bound MTSES molecule would make it more difficult for the MTS reactive sulfur to closely contact the thiol group of the cysteine at position 166 than to react with the cysteine thiol group at the 512 position. This likely creates a rate-limiting step for MTS reagents to modify E166C because altering the charge at the pore entrance (Fig. 6 *C*) or changing the voltage (Fig. 6 *D*)—although significantly altering the on- and off-rates of the binding of MTSES molecules to the pore (16)—does not affect the MTS modification rate of E166C. Thus, even though the reversible MTSES binding to the E166C pore has a higher affinity at more negative potential, the limitation in the final reaction step curtails the success of the modification.

We thank Drs. Robert Fairclough and Crina Nimigean for helpful discussions and critical readings of the manuscript.

This work was supported by a research grant from the National Institutes of Health (GM065447 to T.-Y.C.) and a postdoctoral fellowship from the American Heart Association (to X.-D.Z.).

REFERENCES

1. Chen, T. Y. 2005. Structure and function of CLC channels. *Annu. Rev. Physiol.* 67:809–839.
2. Pusch, M., and T. J. Jentsch. 2005. Unique structure and function of chloride transporting CLC proteins. *IEEE Trans. Nanobioscience.* 4:49–57.
3. Miller, C. 2006. ClC chloride channels viewed through a transporter lens. *Nature.* 440:484–489.
4. Chen, T. Y., and T. C. Hwang. 2008. CLC-0 and CFTR: chloride channels evolved from transporters. *Physiol. Rev.* 88:351–387.
5. Jentsch, T. J. 2008. CLC chloride channels and transporters: from genes to protein structure, pathology and physiology. *Crit. Rev. Biochem. Mol. Biol.* 43:3–36.
6. Accardi, A., and C. Miller. 2004. Secondary active transport mediated by a prokaryotic homologue of ClC Cl^- channels. *Nature.* 427: 803–807.
7. Picollo, A., and M. Pusch. 2005. Chloride/proton antiporter activity of mammalian CLC proteins ClC-4 and ClC-5. *Nature.* 436:420–423.
8. Scheel, O., A. A. Zdebik, …, T. J. Jentsch. 2005. Voltage-dependent electrogenic chloride/proton exchange by endosomal CLC proteins. *Nature.* 436:424–427.
9. Maduke, M., C. Miller, and J. A. Mindell. 2000. A decade of CLC chloride channels: structure, mechanism, and many unsettled questions. *Annu. Rev. Biophys. Biomol. Struct.* 29:411–438.
10. Dutzler, R., E. B. Campbell, …, R. MacKinnon. 2002. X-ray structure of a ClC chloride channel at 3.0 Å reveals the molecular basis of anion selectivity. *Nature.* 415:287–294.
11. Dutzler, R., E. B. Campbell, and R. MacKinnon. 2003. Gating the selectivity filter in ClC chloride channels. *Science.* 300:108–112.
12. Bykova, E. A., X. D. Zhang, …, J. Zheng. 2006. Large movement in the C terminus of CLC-0 chloride channel during slow gating. *Nat. Struct. Mol. Biol.* 13:1115–1119.
13. Lin, C. W., and T. Y. Chen. 2003. Probing the pore of ClC-0 by substituted cysteine accessibility method using methane thiosulfonate reagents. *J. Gen. Physiol.* 122:147–159.
14. Engh, A. M., and M. Maduke. 2005. Cysteine accessibility in ClC-0 supports conservation of the ClC intracellular vestibule. *J. Gen. Physiol.* 125:601–617.
15. Zhang, X. D., Y. Li, …, T. Y. Chen. 2006. Roles of K149, G352, and H401 in the channel functions of ClC-0: testing the predictions from theoretical calculations. *J. Gen. Physiol.* 127:435–447.
16. Zhang, X. D., P. Y. Tseng, …, T. Y. Chen. 2009. Blocking pore-open mutants of CLC-0 by amphiphilic blockers. *J. Gen. Physiol.* 133:43–58.
17. Akabas, M. H., D. A. Stauffer, …, A. Karlin. 1992. Acetylcholine receptor channel structure probed in cysteine-substitution mutants. *Science.* 258:307–310.
18. Lin, Y. W., C. W. Lin, and T. Y. Chen. 1999. Elimination of the slow gating of ClC-0 chloride channel by a point mutation. *J. Gen. Physiol.* 114:1–12.
19. Chen, M. F., and T. Y. Chen. 2003. Side-chain charge effects and conductance determinants in the pore of ClC-0 chloride channels. *J. Gen. Physiol.* 122:133–145.
20. Chen, T. Y., M. F. Chen, and C. W. Lin. 2003. Electrostatic control and chloride regulation of the fast gating of ClC-0 chloride channels. *J. Gen. Physiol.* 122:641–651.
21. Zhang, X. D., and T. Y. Chen. 2009. Amphiphilic blockers punch through a mutant CLC-0 pore. *J. Gen. Physiol.* 133:59–68.
22. Pascual, J. M., and A. Karlin. 1998. State-dependent accessibility and electrostatic potential in the channel of the acetylcholine receptor. Inferences from rates of reaction of thiosulfonates with substituted cysteines in the M2 segment of the α subunit. *J. Gen. Physiol.* 111:717–739.
23. Wilson, G. G., J. M. Pascual, …, A. Karlin. 2000. The intrinsic electrostatic potential and the intermediate ring of charge in the acetylcholine receptor channel. *J. Gen. Physiol.* 115:93–106.

24. Stauffer, D. A., and A. Karlin. 1994. Electrostatic potential of the acetylcholine binding sites in the nicotinic receptor probed by reactions of binding-site cysteines with charged methanethiosulfonates. *Biochemistry*. 33:6840–6849.

25. Osteen, J. D., and J. A. Mindell. 2008. Insights into the ClC-4 transport mechanism from studies of Zn^{2+} inhibition. *Biophys. J.* 95:4668–4675.

26. Pusch, M., U. Ludewig, …, T. J. Jentsch. 1995. Gating of the voltage-dependent chloride channel CIC-0 by the permeant anion. *Nature*. 373:527–531.

27. Chen, T. Y., and C. Miller. 1996. Nonequilibrium gating and voltage dependence of the ClC-0 Cl- channel. *J. Gen. Physiol*. 108:237–250.

28. Woodhull, A. M. 1973. Ionic blockage of sodium channels in nerve. *J. Gen. Physiol*. 61:687–708.